Bioprocess Biosyst Eng (2011) 34:1143–1150
DOI 10.1007/s00449-011-0565-4

ORIGINAL PAPER

Glucose biosensor based on titanium dioxide-multiwall carbon nanotubes-chitosan composite and functionalized gold nanoparticles

Meihe Zhang · Ruo Yuan · Yaqin Chai · Wenjuan Li · Huaan Zhong · Cun Wang

Received: 5 June 2011 / Accepted: 14 June 2011 / Published online: 1 July 2011

Abstract In this paper, a new glucose biosensor was prepared. At first, Prussian blue (PB) was electrodeposited on a glassy carbon electrode (GCE) modified by titanium dioxide-multiwall carbon nanotubes-chitosan (TiO_2-MWNTs-CS) composite, and then gold nanoparticles functionalized by poly(diallyldimethylammonium chloride) (PDDA-Au) were adsorbed on the PB film. Finally, the negatively charged glucose oxidase (GOD) was self-assembled on to the positively charged PDDA-Au. The electrochemical performances of the modified electrodes had been studied by cyclic voltammetry (CV) and amperometric methods, respectively. In addition, the stepwise fabrication process of the as-prepared biosensor was characterized by scanning electron microscopy. PDDA-Au nanoparticles were characterized by ultraviolet–vis absorption spectroscopy and transmission electron microscopy. Under the optimal conditions, the as-prepared biosensor exhibited a good response performance to glucose with a linear range from 6 μM to 1.2 mM with a detection limit of 0.1 μM glucose ($S/N = 3$). In addition, this work indicated that TiO_2-MWNTs-CS composite and PDDA-Au nanoparticles held great potential for constructing biosensors.

Keywords Glucose biosensor · Multiwall carbon nanotubes · Titanium dioxide · Prussian blue · Functionalized gold nanoparticles

Introduction

The accurate and reliable determination of blood glucose level is important for the diagnosis, clinical analysis, and management of diabetes. Since Clark and Lyons [1] reported their enzyme electrode for measuring glucose, numerous methods were developed for this purpose. Among the surface plasmon resonance [2], electrochemical biosensors [3, 4], and other biosensors, the electrochemical biosensors have gained increasing interest for their rapid response, simplicity, high sensitivity, and low cost. The performance of an amperometric glucose biosensor often depends on glucose oxidase (GOD) immobilization technology, so the development of simple and reliable materials for immobilizing GOD is crucial [5, 6]. In order to fabricate excellent biosensors, various materials have been used for immobilizing enzymes. Organic–inorganic composite material for immobilizing enzymes represents one of the most emerging areas of nanotechnology [7]. Organic components benefit the formation of defect-free inorganic membranes and make it less brittle. Organic membranes show good chemical and thermal stability improved by an inorganic phase. For example, chitosan (CS) was usually combined with TiO_2 nanoparticles [8, 9], ZnO nanoparticles [10, 11], and carbon nanotubes [12, 13]. Nowadays, there are few reports about titanium dioxide-multiwall carbon nanotubes-chitosan (TiO_2-MWNTs-CS) composite. This composite showed good biocompatibility, large surface-to-volume ratio, and excellent electron-conductive ability to construct biosensors.

Electronic supplementary material The online version of this article (doi:10.1007/s00449-011-0565-4) contains supplementary material, which is available to authorized users.

M. Zhang · R. Yuan (✉) · Y. Chai · W. Li · H. Zhong · C. Wang
Key Education Ministry Laboratory on Luminescence and Real-Time Analysis, College of Chemistry and Chemical Engineering, Southwest University, Chongqing 400715, China
e-mail: yuanruo@swu.edu.cn

In recent years, metal nanoparticles have attracted considerable attention due to their electrical and attractive physicochemical characteristics. Especially, gold nanoparticles (AuNPs), owing to its good biocompatibility, high surface-to-volume ratio, and excellent ability of transferring electron between biomolecules and electrode surface, have been widely studied to enhance the sensitivity of biosensor [14]. What is more, they can provide more binding sites and congenial microenvironment for biomolecules. However, AuNPs most used were negatively charged and they were easy to aggregate, so the protecting agents such as thiols and polymers are used to circumvent this problem [15]. Especially, poly(diallyldimethylammonium chloride) (PDDA) [16], a positively charged ionic polymer, is used to avoid the aggregation of AuNPs, and positively charged AuNPs can be obtained. This strategy describes a simple, one-step approach to the formation of functionalized gold nanoparticles in which PDDA acts as both reducing and stabilizing agents. Moreover, the positively charged PDDA-Au nanoparticles can be effectively self-assembled onto the negatively charged membrane by electrostatic interaction.

Usually, the detection of glucose is accomplished by monitoring the information of hydrogen peroxide (H_2O_2). However, the direct electrocatalysis of H_2O_2 requires a high working potential. At such potential, the electrochemically active interfering species are easily oxidized, which leads to interfering current [17]. Prussian blue (PB), as a mediator, is an excellent catalyst for H_2O_2 reduction at low potentials, which greatly decreases the interference [18].

In this paper, we aimed to improve the stability and bioactivity of enzyme biosensors and combine the advantageous features of TiO_2-MWNTs-CS composite and PDDA-Au nanoparticles to develop a simple, stable, and sensitive glucose biosensor. The preparation, characterization of the synthesized TiO_2-MWNTs-CS composite and PDDA-Au nanoparticles, as well as the electrochemical properties of biosensor are described in detail. Moreover, the as-prepared biosensor exhibited long-term stability, good reproducibility and high anti-interference ability.

Materials and methods

Reagents and apparatus

Glucose oxidase (E.C. 1.1.3.4, 151,000 unit/g), chlorauric acid ($HAuCl_4 \cdot 4H_2O$), Nano-titanium dioxide (TiO_2, 5%, pH 2–3) were purchased from Sigma (USA). PDDA (20%, w/w in water, molecular weight 20,000) was purchased from Aldrich (USA). All other reagents were of analytical grade and used without further purification.

Cyclic voltammetric (CV) and amperometric experiments were performed with a CHI 600D electrochemical workstation (China). A conventional three-compartment electrochemical cell was employed with use of a modified glassy carbon electrode (GCE) as working electrode, a platinum wire as auxiliary electrode and a saturated calomel electrode as a reference electrode. The image of the stepwise assembly processes of the modified electrode was characterized by scanning electron microscopy (SEM, S-4800, Hitachi, Japan). The ultraviolet–vis (UV–vis) absorption spectra of PDDA-Au were collected on a UV–vis spectrometer (UV–vis 8500). The size of PDDA-Au is estimated from transmission electron microscopy (TEM) (H600, Hitachi Instrument, Japan).

Preparation of TiO_2-MWNTs-CS

2 mg MWNTs was dispersed in 2 mL CS (1 mg/mL in 1% HAc) by ultrasonic agitation. Subsequently, TiO_2 was added to obtain TiO_2 doped MWNTs-CS homogeneous composite. The TiO_2-MWNTs-CS composite was treated for 10 min by ultrasonication before use and stored in 4 °C for future use.

Synthesis of PDDA-Au nanoparticles

The PDDA-Au nanoparticles were synthesized according to Ref. [19]. 250 μL PDDA (4% w/w in water), 40 mL water, 200 μL of 0.5 M NaOH and 100 μL $HAuCl_4$ (1% w/w in water) were added into a beaker. After thoroughly mixed, the solution continued heating until the color changed to red and no further change occurred. An inverted culture dish was covered on the beaker to avoid the reaction liquid vaporized rapidly. The obtained PDDA-Au nanoparticles were very stable, no precipitate had been observed several months later. Figure 1a shows UV–vis spectra of PDDA solution (curve a) with no obvious absorption peak. But PDDA-Au solution (curve b) shows a characteristic absorption center at 526 nm, which is a typical absorption for AuNPs. PDDA–Au nanoparticles are further characterized using TEM. In Fig. 1b, PDDA–Au nanoparticles are almost spherical, and the average diameter is about 8 nm which was fatter than the unmodified Au (Fig. 1c), indicating it was tightly wrapped by PDDA.

Preparation of glucose biosensor (Scheme 1)

The GCE ($\Phi = 4$ mm) was polished with 0.3 and 0.05 μm alumina slurry, and rinsed in ethanol and water by sequential sonication. Then 10 μL TiO_2-MWNTs-CS was dropped onto the bare GCE. After that, the electrodeposition of PB was accomplished in an unstirred fresh aqueous

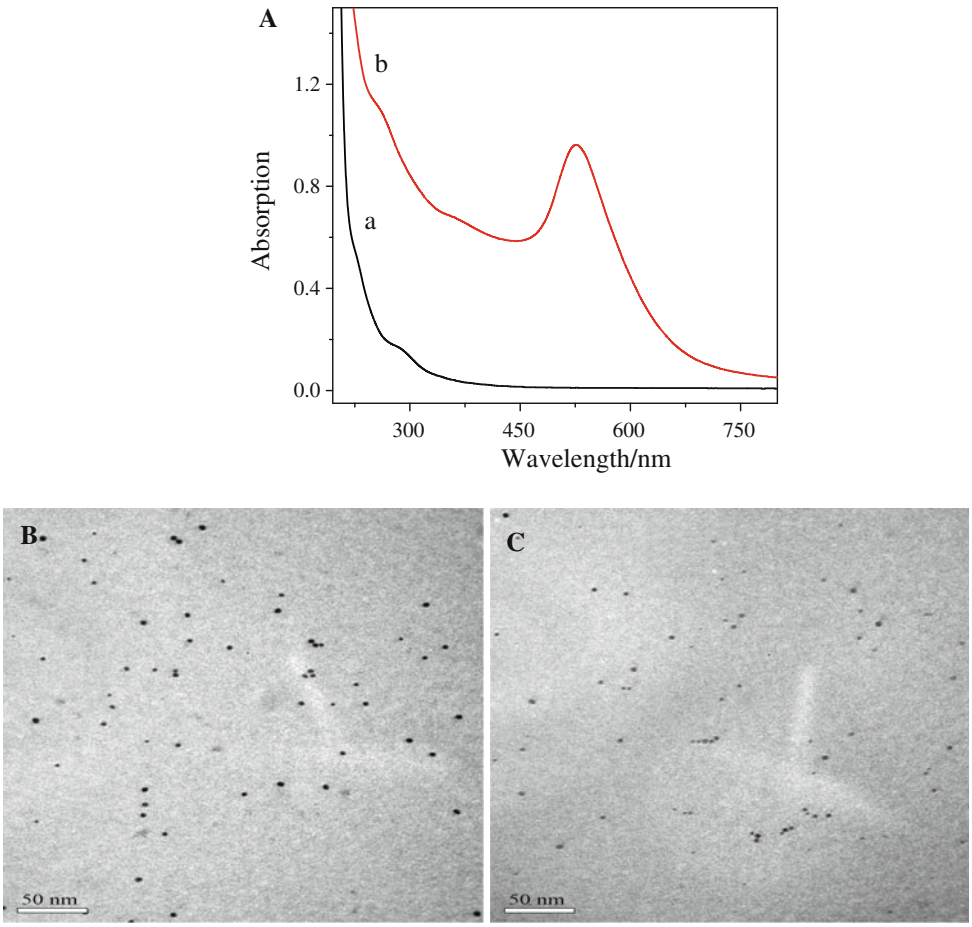

Fig. 1 **a** UV–vis absorption spectrum of PDDA solution (**a**) and PDDA-Au solution (**b**), (**b**) TEM image of the PDDA-Au nanoparticles, and (**c**) TEM image of Au nanoparticles

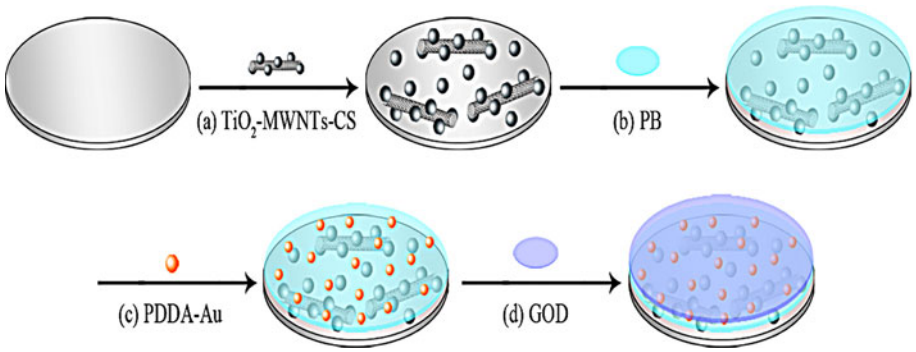

Scheme 1 Illustration of the preparation process for the modified electrode

solution consisting of 2.5 mM $K_3[Fe(CN)_6]$ + 2.5 mM $FeCl_3$ + 0.1 M KCl + 0.1 M HCl at 0.4 V for 60 s according to Ref. [20]. Subsequently, the PB modified electrode was activated in 0.1 M KCl + 0.1 M HCl with CVs scans ranging from −0.05 to 0.35 V. Following that, it was immersed in PDDA-Au solution for 8 h. Finally, 10 μL GOD (6 mg/mL in 0.1 M phosphate buffer saline, pH 7.0) solutions were dropped onto the electrode surface. For comparison, GOD/PDDA-Au/PB/GCE was prepared similarly. The modified electrodes were stored at 4 °C for future use.

Results and discussion

Scanning electron microscopy (SEM) of the modified electrode

SEM was employed to characterize the stepwise fabrication process of the as-prepared biosensor as shown in Fig. 2. Figure 2a shows an image of TiO_2-MWNTs-CS. The TiO_2 was dispersed homogeneously in CS and MWNTs-CS composite, so the TiO_2-MWNTs-CS composite was synthesized successfully. In Fig. 2b when PB

was electrodeposited on the TiO_2-MWNTs-CS film, many PB crystals can be found in the surface of TiO_2-MWNTs-CS composite. As shown in Fig. 2c, after PDDA-Au nanoparticles were adsorbed on the PB/TiO_2-MWNTs-CS membrane, many small bright particles can be observed, indicating that PDDA-Au nanoparticles had been adsorbed successfully. The corresponding SEM image obviously changed after GOD assembling onto the PDDA-Au/PB/TiO_2-MWNTs-CS surface, which demonstrated a lot of GOD immobilized on the PDDA-Au/PB/TiO_2-MWNTs-CS film. On the basic of SEM results, we might conclude that the as-prepared biosensor could preliminarily be applied for determination of glucose.

Electrochemical characterization of biosensor by CV

The electrochemical behavior of the assembly-modified process of the electrodes was monitored by cyclic voltammetry experiments (Fig. 3). No redox peaks were observed at bare GCE as the lack of electron mediator (Fig. 3a). The background current increased after the modification of TiO_2-MWNTs-CS because of the excellent electro-transfer property of MWNTs (Fig. 3b). After PB was electrodeposited on the TiO_2-MWNTs-CS/GCE, a pair of well-defined redox peaks appeared indicating PB possessing excellent redox activity (Fig. 3c). The current of curve d decreased after adsorbing PDDA-Au nanoparticles as compared with curve c. After GOD was loaded onto PDDA-Au/PB/TiO_2-MWNTs-CS/GCE, the peak currents decreased gradually because of GOD hindering the transfer of electrons toward the electrode surface, which indicated that GOD had been immobilized on the electrode surface successfully (Fig. 3e).

Figure 4 shows the CVs of the prepared biosensor in 0.025 M PBS (pH 6.0) at different scan rates. It observes that both anodic and cathodic peak currents increased linearly with the square root of scan rate in the range 10–600 mV/s (inset of Fig. 4), suggesting a diffusion-controlled redox process.

Optimization conditions for glucose detection system

For a biosensor, the pH is very important factor to the electrochemical behavior of the biosensor. Thus, the effect of pH on the biosensor response was investigated by the changes of chronoamperometric current under constant glucose concentration (0.6 mM). As shown in Fig. 5, it was found that the current responses reached the maximum when the value of pH was 6.0. However, as the pH value increased from 6.5 to 8.5, the current decreased. Decrease in the response at high pH was possibly due to the decrease of enzymatic activity. Thus, the buffer solution of pH 6.0 was adopted for further experiments to obtain a high analytical sensitivity.

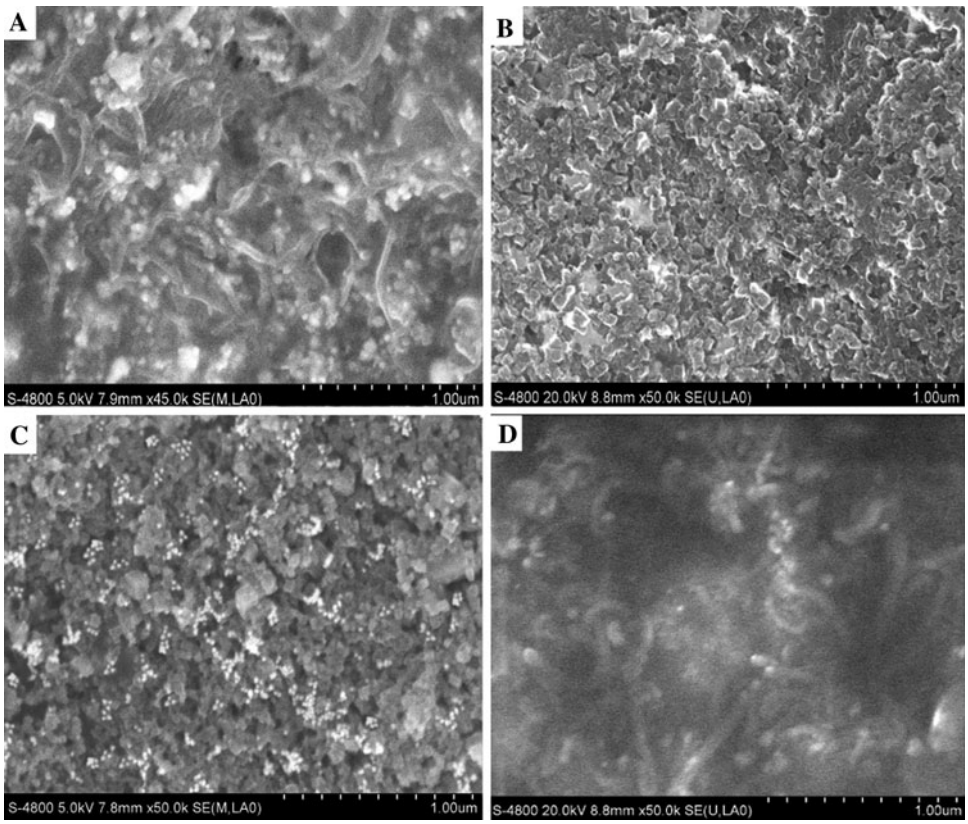

Fig. 2 SEM of TiO_2-MWNTs-CS modified surface (**a**), PB/TiO_2-MWNTs-CS modified surface (**b**), PDDA-Au/PB/TiO_2-MWNTs-CS modified surface (**c**) and GOD/PDDA-Au/PB/TiO_2-MWNTs-CS modified surface (**d**)

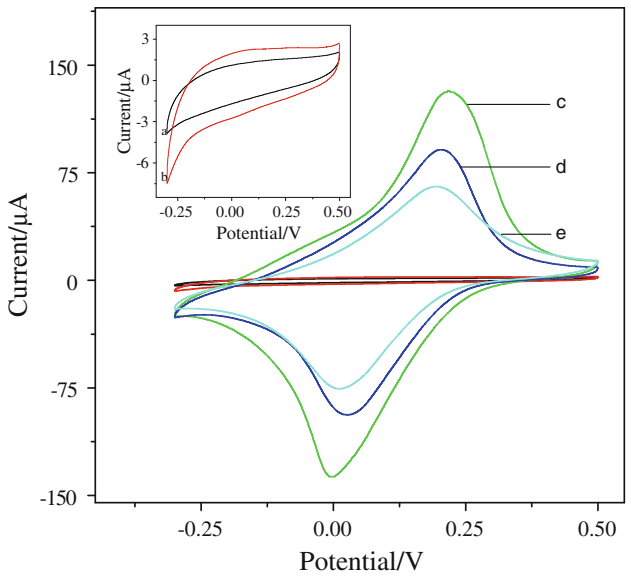

Fig. 3 CVs of bare GCE (**a**), TiO_2-MWNTs-CS/GCE (**b**), PB/TiO_2-MWNTs-CS/GCE (**c**), PDDA-Au/PB/TiO_2-MWNTs-CS/GCE (**d**), GOD/PDDA-Au/PB/TiO_2-MWNTs-CS/GCE (**e**) in 0.025 M phosphate buffer saline (pH 6.0) at 50 mV/s

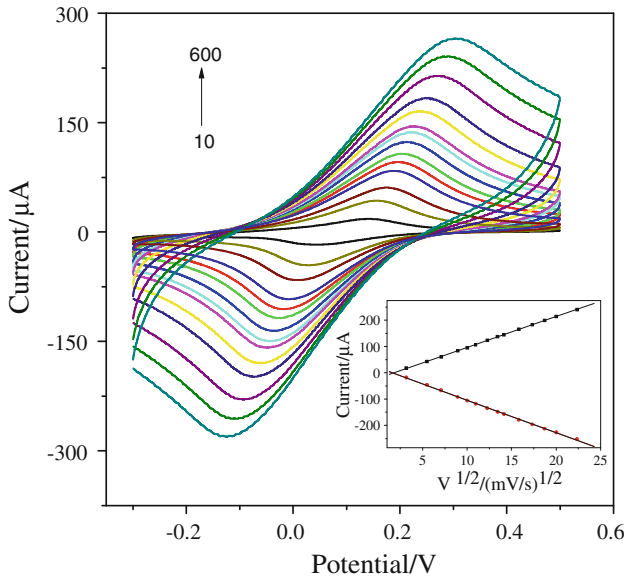

Fig. 4 CVs of the biosensor at different scan rates (from inner to outer): 10, 30, 50, 80, 100, 120, 150, 180, 200, 250, 300, 350, 400, 500, and 600 mV/s in 0.025 M phosphate buffer saline (pH 6.0). *Inset* plot of peak current versus $v^{1/2}$

The effect of applied potential on the biosensor was also investigated in the presence of 0.6 mM glucose (Fig. 6). As can be seen, the amperometric current increased gradually as the applied potential decreased from 0.2 to −0.2 V, but in order to minimize the interference and get enough current responses, −0.1 V was chosen as the working potential.

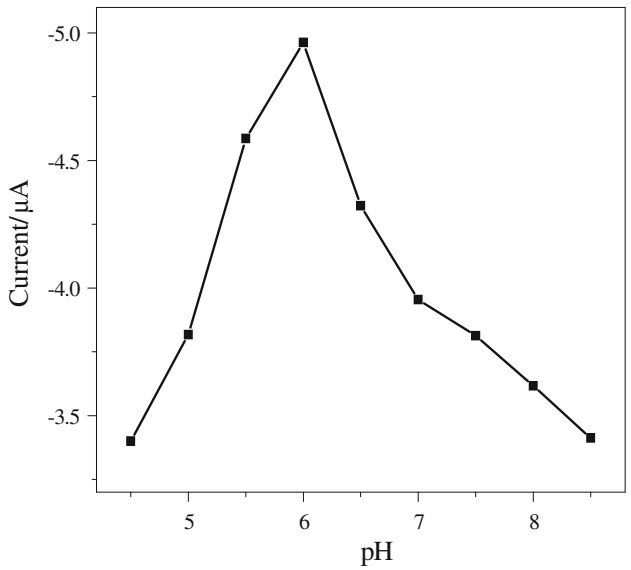

Fig. 5 Effect of pH on the biosensor response to 0.6 mM glucose in 0.025 M phosphate buffer saline at −0.1 V

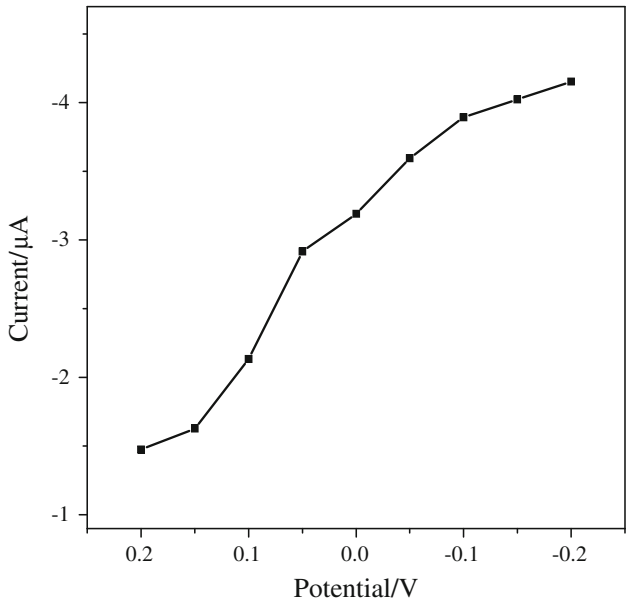

Fig. 6 Effect of potential on the biosensor response to 0.6 mM glucose in 0.025 M phosphate buffer saline (pH 6.0)

The amount of PDDA-Au depended on the adsorbing time. In order to quantitate the amount of PDDA-Au exposed to the electrode, we studied the influence of adsorbing time of PDDA-Au on the performance of the as-prepared biosensor (see Supporting Information Fig. S1), and the adsorbing time of 8 h was adopted in this work.

Amperometric response of the glucose biosensor

The characteristics of the glucose biosensor are investigated by amperometric measurement under optimized

conditions. The typical current-time curve of the biosensor is shown in Fig. 7. Upon each injection of glucose, the rapid increase in currents was observed. This was ascribed to the MWNTs and PDDA-Au nanoparticles on the electrode surface efficiently accelerated the electron transfer. In the inset of Fig. 7, the current response was linear for glucose concentrations in the range of 6 μM to 1.2 mM ($r = 0.999$) with a detection limit of 0.1 μM ($S/N = 3$). The detection limit of 2 μM ($S/N = 3$) is lower then the reported 2.7 μM [21], 3 μM [22], and 5.7 μM [23].

In order to check up the electrochemical responses of TiO_2-MWNTs-CS composite, a comparative study was carried out by using two kinds of biosensor GOD/PDDA-Au/PB/GCE (a) and GOD/PDDA-Au/PB/TiO_2-MWNTs-CS/GCE (b) into a stirred solution of 0.025 M PBS (pH 6.0) at applied potential of −0.1 V with injecting the same concentration of glucose. As shown in Fig. 8, the biosensor using TiO_2-MWNTs-CS composite showed a better amperometric response. The reason was that the favorable microenvironment provided with CS for keeping the activity of GOD, and the high surface area provided with MWNTs for increasing the immobilization amount of GOD and facilitated electrons transfer to electrode surface, thus the biosensor showed a much better electrocatalytic performance for glucose.

The response mechanism of the glucose biosensor

The mechanism involved in the detection of glucose with generation of H_2O_2 occurs as the following:

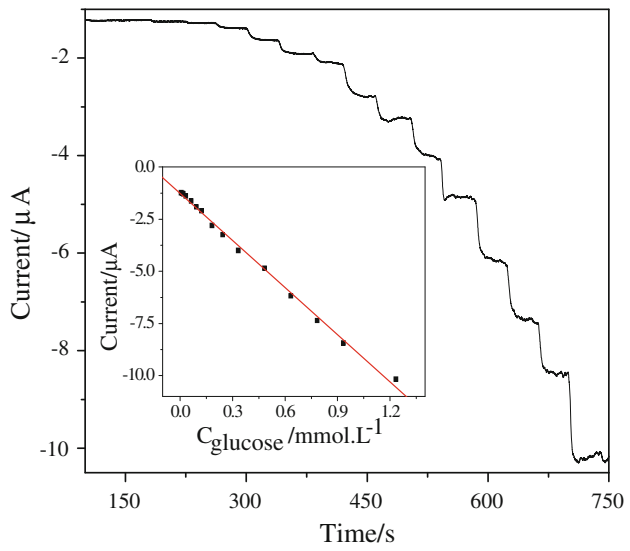

Fig. 7 Amperometric response of the biosensor to successive addition of glucose into a stirring 0.025 mM phosphate buffer saline (pH 6.0) at −0.1 V. *Inset* shows the linear calibration curve

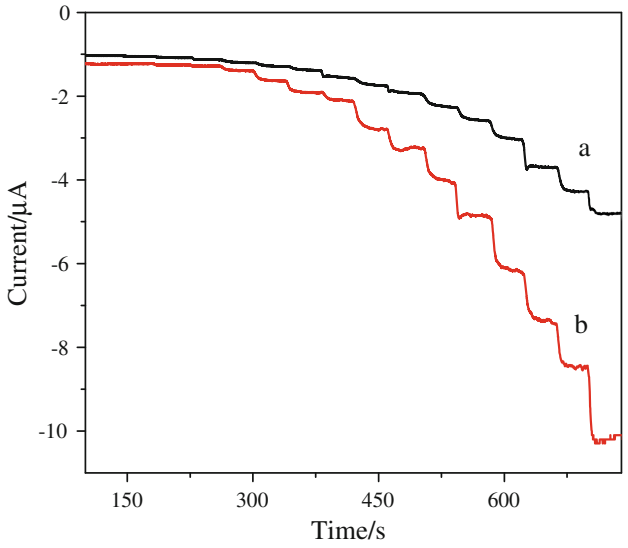

Fig. 8 Amperometric response of the biosensor to successive adding of glucose by GOD/PDDA-Au/PB/GC (**a**) and GOD/PDDA-Au/PB/TiO_2-MWNTs-CS/GCE (**b**) into a stirring 0.025 M phosphate buffer saline (pH 6.0) at −0.1 V

$$\text{Glucose} + \text{GOD (FAD)} \rightarrow \text{gluconolactone} + \text{GOD (FADH}_2\text{)} \quad (1)$$

$$\text{GOD (FADH}_2\text{)} + \text{O}_2 \rightarrow \text{GOD (FAD)} + \text{H}_2\text{O}_2 \quad (2)$$

$$\text{K}_2\text{Fe}^{2+}\text{Fe}^{2+}(\text{CN})_6(\text{PW}) \overset{\text{H}_2\text{O}_2}{\underset{\text{e}}{\rightleftharpoons}} \text{KFe}^{3+}\text{Fe}^{2+}(\text{CN})_6(\text{PB}) + \text{K}^+ \quad (3)$$

The glucose is oxidized by GOD (Eq. 1) and GOD is returned to its original active state (Eq. 2), with formation of gluconolactone and H_2O_2. The amount of H_2O_2 produced is directly proportional to the concentration of glucose. Then PB provides a high catalytic for the reduction of H_2O_2. So H_2O_2 can be detected quantitatively on the modified electrode.

Reproducibility and stability of the glucose biosensor

The relative standard deviation (RSD) of the biosensor response to 0.6 mM glucose was 1.2% for 10 successive measurements, which displayed an acceptable reproducibility. The stability of the biosensor was also tested. After 1 week, the current response decreased 6.8% of its initial response, and 16.6% after 2 weeks. So the prepared biosensor shows an acceptable stability, which can be attributed to the two aspects. On the one hand, TiO_2-MWNTs-CS, PB, and PDDA-Au nanoparticles on the electrode surface were very stable. On the other hand, TiO_2-MWNTs-CS composite provided a friendly environment for GOD, which maintained

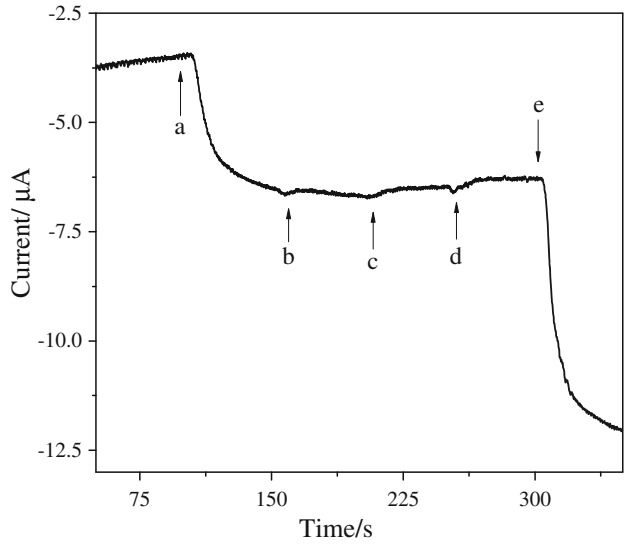

Fig. 9 Effect of the possible interferents in biosensor. The *arrows* show the each moment at the injection of the interfering compounds: (**a**) 0.3 mM glucose, (**b**) 1 mM glycin, (**c**) 1 mM L-cysteine, (**d**) 1 mM dopamine, (**e**) 0.6 mM glucose in a stirring 0.025 M phosphate buffer saline (pH 6.0) at −0.1 V

Table 1 Recoveries of glucose by the biosensor

Sample	$C_{original}$ (mM)	C_{added} (mM)	$C_{detected}$ (mM)	Recovery (%)
1	0.09	0.06	0.141	94
2	0.15	0.12	0.282	104.4
3	0.6	0.3	0.887	98.5

C concentration of glucose

the bioactivity of GOD and prolonged the life of the biosensor.

Selectivity of the glucose biosensor

Figure 9 represents the amperometric responses of glucose in the presence of glycine, L-cysteine, and dopamine. The current generated from the interfering species was negligible thus indicating that the biosensor had a strong anti-interference ability. Obviously, the higher selectivity of the biosensor was attributed to a low operating potential, and the efficient and selective mediator by PB.

Recovery experiment

The analytical applicability of the biosensor was evaluated by the standard addition method. Table 1 listed the recovery of three samples of different glucose concentrations. The recovery rate was between 94 and 104.4%. The satisfying results demonstrated that the biosensor had a great potential for practical application.

Conclusions

In summary, we had demonstrated the applicability of the biosensor for detecting glucose based on TiO_2-MWNTs-CS, PB, and PDDA-Au. The as-prepared biosensor offered several advantages as follows. Firstly, TiO_2-MWNTs-CS provided better environment for the efficient enzyme loading and maintenance of the enzymatic bioactivity in order to increase the sensitivity of the biosensor. Secondly, high surface area and a biocompatible microenvironment provided by the PDDA-Au facilitated higher enzyme loading and helped enzyme to retain its bioactivity, respectively. Based on these advantages, the as-prepared biosensor exhibited excellent sensitivity, selectivity, and good stability. Moreover, this method can be used in the preparation of other amperometric enzyme biosensors.

Acknowledgments The National Natural Science Foundation of China (21075100), the Ministry of Education of China (Project 708073), the Nature Science Foundation of Chongqing City (CSTC-2009BA1003), Specialized Research Fund for the Doctoral Program of Higher Education (20100182110015), State Key Laboratory of Electroanalytical Chemistry (SKIEAC 2010009), the 211 Project of Southwest University (the Third Term) and the High Technology Project Foundation of Southwest University (XSGX 02), China supported this work.

References

1. Leland C, Clark Jr, Lyons Champ (1962) Electrode systems for continuous monitoring in cardiovascular surgery. Ann NY Acad Sci 102:29–45
2. Deng CY, Li MR, Xie QJ, Liu ML, Yang Q, Xiang CH, Yao SZ (2007) Construction as well as EQCM and SECM characterizations of a novel Nafion/glucose oxidase-glutaraldehyde/poly(thionine)/Au enzyme electrode for glucose sensing. Sensor Actuat B Chem 122:148–157
3. Liu SQ, Wang KW, Du D, Sun YM, He L (2007) Recognition of glycoprotein peroxidase via Con A-carrying self-assembly layer on gold. Biomacromolecules 8:2142–2148
4. Cao X, Wang N (2010) A novel non-enzymatic electrochemical glucose sensor modified with FeOOH nanowire. Electrochem Commun 12:1581–1584
5. Subbiah A, Liu C, Ashok K, Li CZ (2010) Enzyme-doped grapheme nanosheets for enhanced glucose biosensing. J Phys Chem C 114(30):12920–12924
6. Bayramoglu G, Altıntas B, Arıca MY (2011) Reversible immobilization of uricase on conductive polyaniline brushes grafted on polyacrylonitrile film. Bioprocess Biosyst Eng 34: 127–134
7. Wang ZJ, Yang YH, Li JS, Gong JL, Shen GL, Yu RQ (2006) Organic–inorganic matrix for electrochemical immunoassay: detection of human IgG based on ZnO/chitosan composite. Talanta 69:686–690
8. Zhou N, Yang T, Jiao K, CX S (2010) Electrochemical deoxyribonucleic acid biosensor based on multiwalled carbon nanotubes/Ag-TiO_2 composite film for label-free phosphinothricin acetyltransferase gene detection by electrochemical impedance spectroscopy. Chinese J Anal Chem 38(3):301–306

9. Zhu YH, Cao HM, Tang LH, Yang XL, Li CZ (2009) Immobilization of horseradish peroxidase in three-dimensional macroporous TiO_2 matrices for biosensor applications. Electrochim Acta 54:2823–2827
10. Liu Y, Chu ZY, Jin WQ (2009) A sensitivity-controlled hydrogen peroxide sensor based on self-assembled Prussian Blue modified electrode. Electrochem Commun 11:484–487
11. Li LH, Deng JC, Deng HR, Liu Zl, Xin L (2010) Synthesis an characterization of chitosan/ZnO nanoparticle composite membranes. Carbohyd Res 345:994–998
12. Kang XH, Mai ZB, Zou XY, Cai PX, Mo JY (2007) A novel glucose biosensor based on immobilization of glucose oxidase in chitosan on a glassy carbon electrode modified with gold–platinum alloy nanoparticles/multiwall carbon nanotubes. Anal Biochem 369:71–79
13. Li A, Yuan R, Chai YQ, Chen SH, An HZ (2008) Sensitive immunoassay of human chorionic gonadotrophin based on multiwalled carbon nanotube–chitosan matrix. Bioprocess Biosyst Eng 31:551–558
14. Zhuo Y, Yuan PX, Yuan R, Chai YQ, Cheng LH (2009) Bienzyme functionalized three-layer composite magnetic nanoparticles for electrochemical immunosensors. Biomaterials 30:2284–2290
15. Sun XP, Dong SJ, Wang EK (2004) One-step preparation and characterization of poly(propyleneimine) dendrimer-protected silver nanoclusters. Macromolecules 19:7105–7108
16. Chen HJ, Wang YL, Wang YZ, Dong SJ, Wang EK (2006) One-step preparation and characterization of PDDA-protected gold nanoparticles. Polymer 47:763–766
17. Wu BY, Hua SH, Yin F, Li J, Zhao ZX, Huang JD, Chen Q (2007) Amperometric glucose biosensor based on layer-by-layer assembly of multilayer films composed of chitosan, gold nanoparticles and glucose oxidase modified Pt electrode. Biosens Bioelectron 22:838–844
18. Shi HB, Yang Y, Huang JD, Zhao ZX, Xu XH, Anzai JI, OsaT ChenQ (2006) Amperometric choline biosensors prepared by layer-by-layer deposition of choline oxidase on the Prussian blue-modified platinum electrode. Talanta 70:852–858
19. Ma LP, Yuan R, Chai YQ, Chen SH (2009) Amperometric hydrogen peroxide biosensor based on the immobilization of HRP on DNA-silver nanohybrids and PDDA-protected gold nanoparticles. J Mol Catal B Enzym 56:215–220
20. Song ZJ, Yuan R, Chai YQ, Yin B, Fu P, Wang JF (2010) Multilayer structured amperometric immunosensor based on gold nanoparticles and Prussian blue nanoparticles/nanocomposite functionalized interface. Electrochim Acta 55:1778–1784
21. Luo XL, Xu JJ, Du Y, Chen HY (2004) A glucose biosensor based on chitosan–glucose oxidase–gold nanoparticles biocomposite formed by one-step electrodeposition. Anal Biochem 334:284–289
22. Wen D, Zou XQ, Liu Y, Shang L, Dong SJ (2009) Nanocomposite based on depositing platinum nanostructure onto carbon nanotubes through a one-pot, facile synthesis method for amperometric sensing. Talanta 79:1233–1237
23. Pang XY, He DM, Luo SL, Cai QY (2009) An amperometric glucose biosensor fabricated with Pt nanoparticle-decorated carbon nanotubes/TiO_2 nanotube arrays composite. Sens Actuators B 137:134–138